(U) Wind Noise Measurements of Microphones Embedded in the Airfoil of an UAV

October 2012

Wayne E. Prather and William G. Frazier

National Center for Physical Acoustics
University of Mississippi
University, MS
38677

ABSTRACT

Interest in using acoustics as a sensing modality on both stationary and in motion aerial platforms has been increasing in recent years. Embedding microphones in the skin of an airfoil is one option for how acoustic sensors might be employed on a small Unmanned Aerial Vehicle (UAV). The analysis of wind noise measurements made by an array of microphones embedded in the airfoil of a small UAV will be presented. Of particular interest in the acoustic measurements was the level and structure of the wind noise as well as correlation lengths as a function of frequency for directions in line and perpendicular to the predominate direction of the flow. The results and analysis of the measurements will be presented. Additionally, implications for acoustic sensing from aerial platforms will be discussed.

Report Documentation Page

Form Approved
OMB No. 0704-0188

1. REPORT DATE	2. REPORT TYPE	3. DATES COVERED
OCT 2012	**N/A**	**-**

4. TITLE AND SUBTITLE	5a. CONTRACT NUMBER
Wind Noise Measurements of Microphones Embedded in the Airfoil of an UAV	5b. GRANT NUMBER
	5c. PROGRAM ELEMENT NUMBER
6. AUTHOR(S)	5d. PROJECT NUMBER
	5e. TASK NUMBER
	5f. WORK UNIT NUMBER
7. PERFORMING ORGANIZATION NAME(S) AND ADDRESS(ES) **National Center for Physical Acoustics University of Mississippi University, MS 38677**	8. PERFORMING ORGANIZATION REPORT NUMBER
9. SPONSORING/MONITORING AGENCY NAME(S) AND ADDRESS(ES)	10. SPONSOR/MONITOR'S ACRONYM(S)
	11. SPONSOR/MONITOR'S REPORT NUMBER(S)

12. DISTRIBUTION/AVAILABILITY STATEMENT
Approved for public release, distribution unlimited

13. SUPPLEMENTARY NOTES
See also ADM202976. 2012 Joint Meeting of the Military Sensing Symposia (MSS) held in Washington, DC on October 22-25, 2012.

14. ABSTRACT
Interest in using acoustics as a sensing modality on both stationary and in motion aerial platforms has been increasing in recent years. Embedding microphones in the skin of an airfoil is one option for how acoustic sensors might be employed on a small Unmanned Aerial Vehicle (UAV). The analysis of wind noise measurements made by an array of microphones embedded in the airfoil of a small UAV will be presented. Of particular interest in the acoustic measurements was the level and structure of the wind noise as well as correlation lengths as a function of frequency for directions in line and perpendicular to the predominate direction of the flow. The results and analysis of the measurements will be presented. Additionally, implications for acoustic sensing from aerial platforms will be discussed.

15. SUBJECT TERMS

16. SECURITY CLASSIFICATION OF:			17. LIMITATION OF ABSTRACT	18. NUMBER OF PAGES	19a. NAME OF RESPONSIBLE PERSON
a. REPORT	b. ABSTRACT	c. THIS PAGE			
unclassified	**unclassified**	**unclassified**	**SAR**	**13**	

1.0 Introduction

Ground based acoustic arrays are currently being used in a variety of military situations to detect objects of interest that have the one requirement that they make noise. Acoustic arrays can also be used to track the detected object over time as well as identify it. These same capabilities can be afforded by placing an acoustic array on an aerial platform such as an unmanned aerial vehicle (UAV). Although an aerial based acoustic array can offer the same benefits as ground based systems there are several additional benefits as well as issues that are unique to this implementation. These benefits and issues are presented and discussed in this report. The main goal of the effort was to understand the capabilities afforded with airborne acoustic arrays by determining baseline noise floors for an optimized system.

2.0 Airborne Arrays

2.1. Benefits of airborne acoustic arrays

The main benefit of airborne acoustic arrays is associated with the upward refraction of sound during the daytime due to solar heating of the ground. The heating of the earth's surface affects the temperature of the air in contact with the ground causing an air temperature that decreases with height above the ground. In this condition as sound propagates away from a source its path is bent upward leaving minimal acoustic energy reaching ground based acoustic sensors at large distances. Airborne sensors do not suffer from this phenomenon for obvious reasons. For aerial platforms in motion the coverage area of the acoustic array is also larger than a ground based system.

Airborne acoustic sensor arrays also offer additional benefits. For example, the processed track of a detected object of interest can be compared to the known path of the host platform to determine whether the detected object and the host platform are potentially on a collision course. Acoustic sensors are also able to penetrate foliage or deceptive coverings due to the fact that sound travels through and around these types of objects with minimal attenuation. Another benefit is that the presence of acoustic sensors increases the situational awareness of the host vehicle in that it has the capability to "hear" what is going on around it.

2.2. Issues associated with airborne acoustic arrays

The main issue with acoustic sensors used in battlefield applications is wind noise. This is especially true when the platform is in motion such as is the case when the array is placed on an UAV. The signal measured by the acoustic sensors contains some level of noise which directly affects the range of detectability for a specific object of interest. Any decrease in the noise results in an increase in the amount of acceptable attenuation of the signal before it sinks below a minimum detectable signal to noise ratio (SNR). Because the main cause of attenuation of a propagating acoustic signal is spherical spreading the amount of attenuation is directly tied to the distance between the source and receiver. Therefore, if the noise floor is reduced the minimum detectable level is reduced which translates into a larger maximum detectable range.

Because wind noise is the dominant contributor to the measured noise of the system it is the limiting factor on the maximum detectable range of the system. Wind noise is actually a conglomerate of several different phenomena which can roughly be grouped into two different categories. The first category consists of noise that is inherent in the medium of propagation which for these types of efforts is the atmosphere. The atmosphere contains varying amounts of vortices or "eddies" which due to their motion result in fluctuations in the local atmospheric pressure. These fluctuations are measured by the microphone since it is a pressure transducer by definition. An acoustic propagating wave is also small perturbations to the local atmospheric pressure therefore the two are indistinguishable by the sensor on a basic level. The only real difference between the two pressure fluctuations is the speed at which they travel past the sensor. The atmospheric eddies travel past the sensor at the mean wind speed as referenced to the local coordinate system of the sensor. The acoustic wave travels past the sensor at the speed of

sound plus the component of the mean wind speed in the direction of the propagating wave. Some common numbers for these speeds are 343 m/sec for the speed of sound and 10 m/sec for a mean wind speed.

The second category consists of pressure fluctuations resulting from the physical presence of the sensor and the airframe in the flow. These pressure fluctuations are the turbulence that results from the interaction of the flow with the bodies of the airframe and the sensor. The measured noise from the flow body interaction is composed of two parts. The first is the pressure fluctuations which result from flow interactions with the structure producing turbulence which is physically convected across the sensor and directly measured. The second is aeroacoustic born pressure waves that are launched from the flow interaction and travel to the sensor. Windscreen design for rapidly moving aerial platforms begins with the goal of minimizing the component of the measured noise that is due to flow over the physical sensor because these pressure fluctuations are local to the sensor and are therefore directly coupled to the sensing element.

Another issue is associated with the inability to employ spatial averaging due to the impracticality of placing a sensor windscreen design in the flow with dimensions large enough to effect spatial averaging at the frequencies of interest. Microphones in low speed flow typically utilize large foam spherical windscreens that average the pressure over the surface of the windscreen as analyzed by Morgan and Raspet (1992). Because the pressure fluctuations that define the eddies are incoherent they average to zero if a large enough area is covered. For a given windscreen diameter the dividing area between effectiveness and ineffectiveness is defined by eddies whose dimensions are equal to the diameter of the windscreen. Pressure fluctuations from Eddies whose dimensions are much less than the diameter of the windscreen are going to be effectively averaged out and those from eddies much larger are not. The range defined by eddies with dimensions similar to the diameter of the windscreen is defined by a more complicated transition between these two extremes. It is worth noting for clarity that when the spectrum of the noise is considered the frequencies corresponding roughly to each eddy size are defined by the mean wind speed and not the speed of sound as the speed of propagation. This description is simplistic and the reference should be consulted for greater details.

3.0 Test Platform Noise Considerations

3.1. Aeroacoustic Noise Prediction Literature Review

Three particular reports serve as a good starting point for a literature review on aeroacoustic noise prediction, and are excellent summaries of the work to date for each report. These are the NASA Technical Note by Hardin *et al.* (1975), the book chapter by Crighton (1991), and an article by Lilley (2001). These reports suggested that for the glider sensor platform under current consideration, there would be three noise sources that might be significant: trailing edge noise, edge noise from deployed control and lift surfaces such as ailerons, flaps, and slats, and the noise produced by the turbulent boundary layer on the aircraft itself. However, it is assumed that in the data acquisition portion of the flight of interest, the UAV would be in a "clean" configuration with ailerons deflected by only small amounts or not at all, so this noise source was not investigated. Other reports suggest that the turbulent boundary layer itself is a very weak generator of sound. Studies by Willmarth (1958, 1959) showed that an acoustic sensor mounted on a flat plate could only "hear" the turbulent boundary layer if the turbulent boundary layer was passing over the sensor. If the laminar boundary layer was tripped such that a turbulent flow was generated which passed adjacent to but not directly over the sensor, the signal obtained was no different from that of the laminar boundary layer with no turbulent flow present. Thus this potential noise source also was not investigated directly. This leaves the trailing edge noise as the dominant component worth considering for these efforts.

One area of assumed relevance to these efforts that is not addressed in the literature to any major extent is airframe noise due to turbulent inflow. There is some evidence, e.g. Moriarty (2003), particularly from investigations into wind turbine noise, that inflow turbulence can potentially be a dominant noise source. However, most of the wind turbine applications are near ground level where atmospheric boundary layer turbulence might be expected to be more prevalent. Airfoils with sharp leading edges in turbulent flow conditions would tend to be more susceptible to noise due to inflow turbulence. Although most references that discuss airframe noise do not highlight this noise source as a major factor, the present study could not completely resolve the question of the overall significance of inflow turbulence noise for the low speed, relatively low altitude UAV application being considered here.

3.2. Near and Far Field

The vast majority of the analytical work found in the literature is concerned with a far-field analysis of the noise produced by airframes. This research is primarily driven by the "flyover" noise problem associated with aircraft take-off and landing noise. In the current work, however, because the sensor is to be mounted in the airfoil of the aircraft, it is assumed that knowledge of the near-field noise production will be required. One of the first orders of business, then, is to determine what constitutes "near" and "far." The requirement for the far-field assumptions to be correct, according to Lighthill (1978) is that $kr >> 1$, where k is the wavenumber of the sound wave ($k = 2\pi/\lambda$) and r is the radial distance from the source to the observer. The wavelength of the wave is given by λ. The frequency range in question is $10 \text{ Hz} < f < 1000 \text{ Hz}$. Using the assumption that "much less than" can be approximated by a factor of 20 and the value of $c = 1{,}116$ ft/s for the standard sea level speed of sound, the values of r for which the far-field assumption may be assumed to be valid may be calculated from

$$\lambda = \frac{c}{f}, \quad r = \frac{10\lambda}{\pi} \tag{1}$$

Values of wavelength and radius are tabulated below. It appears that for all frequencies of interest the sensors mounted in the airfoil of the aircraft will still be in the near field of the airframe noise sources, assuming a 0.5 ft separation distance between the sensors and the trailing edge.

Table 1 – Frequency, Wavelength, Radius Relationship

f (Hz)	λ (ft)	r (ft)
1000	1.12	3.57
500	2.23	7.1
100	11.16	35.52
10	111.6	355.23

To this point the goal of finding a reliable theoretical technique for predicting and scaling near-field noise from low speed aircraft has not been achieved. Near-field analyses are very rare, and where they are predicted using theory, they tend to be for simplified, two-dimensional geometries (such as airfoils) and for problems which have analytic solutions available (e.g. the sinusoidal gust problem). Indeed, as pointed out by several investigators, it is the recognition that aircraft engine noise had been reduced to levels comparable to airframe noise that drove much of the current research in airframe noise, and in particular trailing edge noise. It might be possible to extend some of the methods found, such as the analytic solutions by Farassat and co-workers, to solve the near-field problem currently at hand. The other alternative is to follow the lead of a number of investigators and obtain a computational fluid dynamics (CFD) solution that couples the flow past the airframe with the noise produced by the airframe, and solve the two problems simultaneously.

3.3. Analytical Results

Lockard (2004) presents a less sophisticated empirical algorithm for far-field trailing edge noise prediction that appears to correlate with a wide range of aircraft size and speed ranges. Defining the overall sound pressure level (OASPL) as

$$OASPL = 10\log_{10}\frac{I\left(Watts/m^2\right)}{I_{ref}} = 120 + 10\log_{10} I\left(Watts/m^2\right) \qquad (2)$$

where $I\left(Watts/m^2\right)$ is the noise intensity and $I_{ref} = 10^{-12}\left(Watts/m^2\right)$. Lockard shows that for a wide range of aircraft in the clean configuration and low to moderate lift coefficients,

$$I\left(Watts/m^2\right) = K\left(\frac{WV_\infty M_\infty^2}{\overline{C}_L H^2}\right). \qquad (3)$$

W is the aircraft weight in Newtons, V_∞ is the free stream velocity in meters per second and H is the distance in meters to an observer directly beneath the aircraft. Because W divided by the coefficient of lift is proportional to the velocity squared, this equation preserves the V^5 relationship predicted for trailing edge broadband noise. Although the coefficient, K, varies with Reynolds number, one can make the simplifying assumption that K is constant and collapse the empirical data reasonably well for a wide range of aircraft weights. For pre-1980 aircraft, Lockard presents a value K of 5.60E-07, whereas for post-1980 aircraft the value of K used by Lockard is 6.30E-08. Although these relationships would not be expected to accurately predict the near-field noise for a sensor embedded in a glider wing, some insight might be gained in looking at the OASPL predicted by the equation above for the weight and speed range of the type of aircraft being considered in this report. Figure 1 depicts the calculations for the 1900 pound Caproni manned sailplane (K = 5.60E-07) and a 35 pound 1/3 scale ASH-26E unmanned sailplane (K = 6.30E-08) at an observer distance of 100 feet below the sailplane as a function of airspeed in knots. Also included on the graph is some measured data from the Caproni sailplane also at a distance of 100 feet.

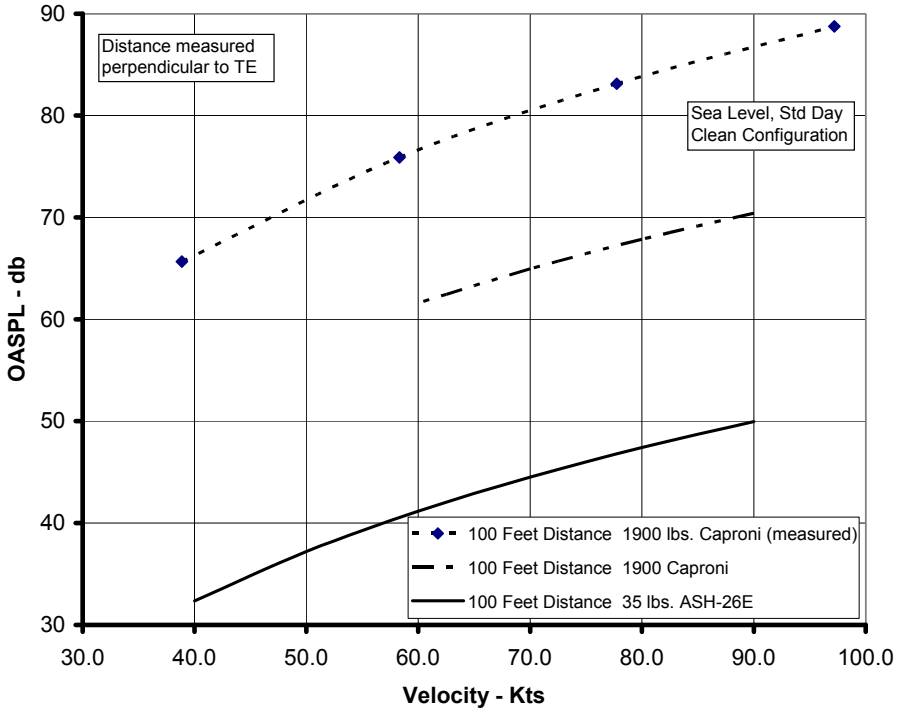

Figure 1. Semi empirical prediction of OASPL from trailing edge noise

3.4. Design Considerations

Based on the scaling laws for far-field noise (V^5, weight^1) the results point to low-speed, ultra-light aircraft to minimize the noise signature from the airframe. Although this conclusion may appear intuitively obvious from the body of evidence in the literature, the role that speed and mass play in airframe noise cannot be overstated in any tradeoff analysis. The speed conclusion is not restricted to the airframe itself but is should also be applied to the propeller for propeller driven platforms.

Other specific design considerations for minimal airframe noise include avoidance of sharp leading edge airfoils to reduce susceptibility to low-frequency noise interaction with turbulent inflow and the avoidance of blunt trailing edges to reduce the potential for tonal noise being generated by vortical shedding from the blunt trailing edge. General design practices that should be adhered to for airframe noise reduction include good gap seals to avoid cavity noise, elimination of all non-essential protuberances and elimination to the maximum practical extent any areas of separated flow on the airframe through efficient airframe contour design and boundary layer control. Most design practices that are aimed at producing extremely efficient or low drag airframes would also be efficient in reducing many of the noise sources that might be present on an airframe in flight. Because sailplanes meet these requirements due to their high aspect wing ratio design and exacting detail to anything that will increase efficiency they were chosen as the best class of airframes to pursue. They were also chosen because of their lack of dependence on a propulsion system to sustain flight. This was due to the desire to eliminate the high levels of noise produced by engines and propellers.

4.0 Test Bed Airframe

4.1. Airframe

Based on the recommendations stated above an airframe was chosen with the additional requirement being that it be available in the general market and not require a custom design. The chosen airframe is a flying wing based glider in which there effectively is no fuselage, a concept arguably made most famous by the Horten brothers in Germany and the Northrop Grumman B-2 Spirit. The goal was to study acoustic sensors embedded in a clean standard section of airfoil so during fabrication the wing was separated along the longitudinal axis and a section of airfoil was placed in the middle within which the data collection system and acoustic sensors were mounted. A rendering of the flying wing can be seen in figure 2 below. The wingspan for the wing is 76", the chord of the center section is 14.5" and the width of the center section is 16". The basic airframe is an Eye Lift 60 radio control airplane kit purchased from www.flyingfoam.com.

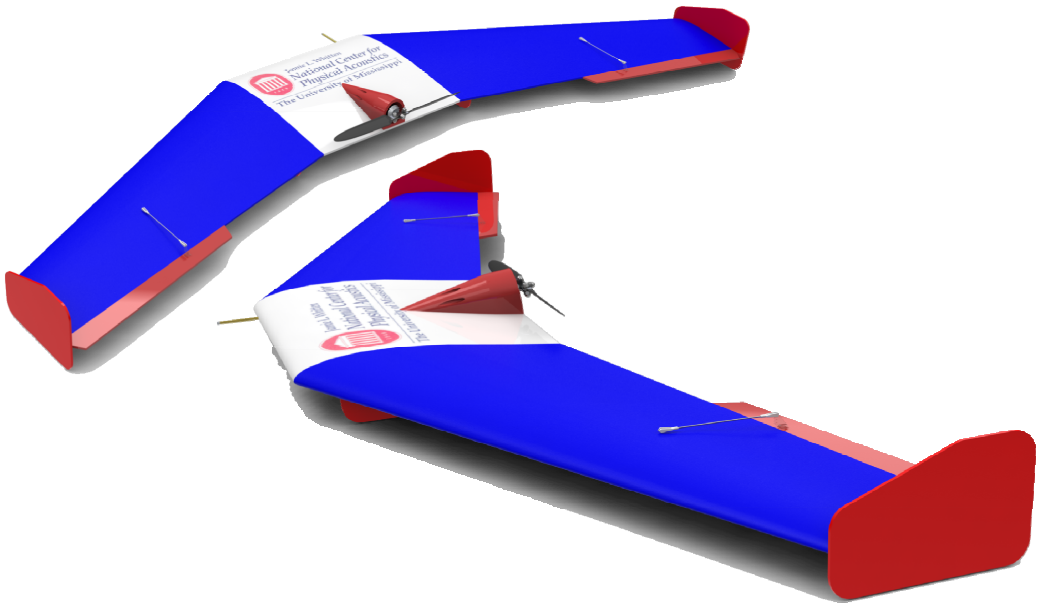

Figure 2. Flying wing test bed airframe

The airfoil for the center section was chosen with several goals in mind. First, the flow over the airfoil needed to remain laminar under the expected conditions of flight which were benign maneuvers and airspeeds not exceeding 25 meters per second. A second goal being that the variations in the coefficient of pressure (Cp) versus variations in the angle of attack be minimal over a large enough spatial area to incorporate the embedded acoustic array. This minimal variation in Cp for variations in angle of attack is critical because this variation in Cp is directly measured by the acoustic sensors in that they are in essence pressure sensors. Because the variations in pressure due to variations in angle of attack are on the order of pounds per square inch (psi) and the acoustic signal pressure is on the order of Pascals it does not take much Cp variance to swamp an acoustic signal. In figure 3 a plot of Cp versus X for an angle of attach of 6 degrees and a Reynolds number of 200,000 can be seen for the chosen airfoil *Sipkill Derivative 11.9 Percent*. The intent was to embed the acoustic sensors on the bottom of the airfoil and it can be seen that the pressure distribution on the bottom side is fairly constant over a large range and is low in level.

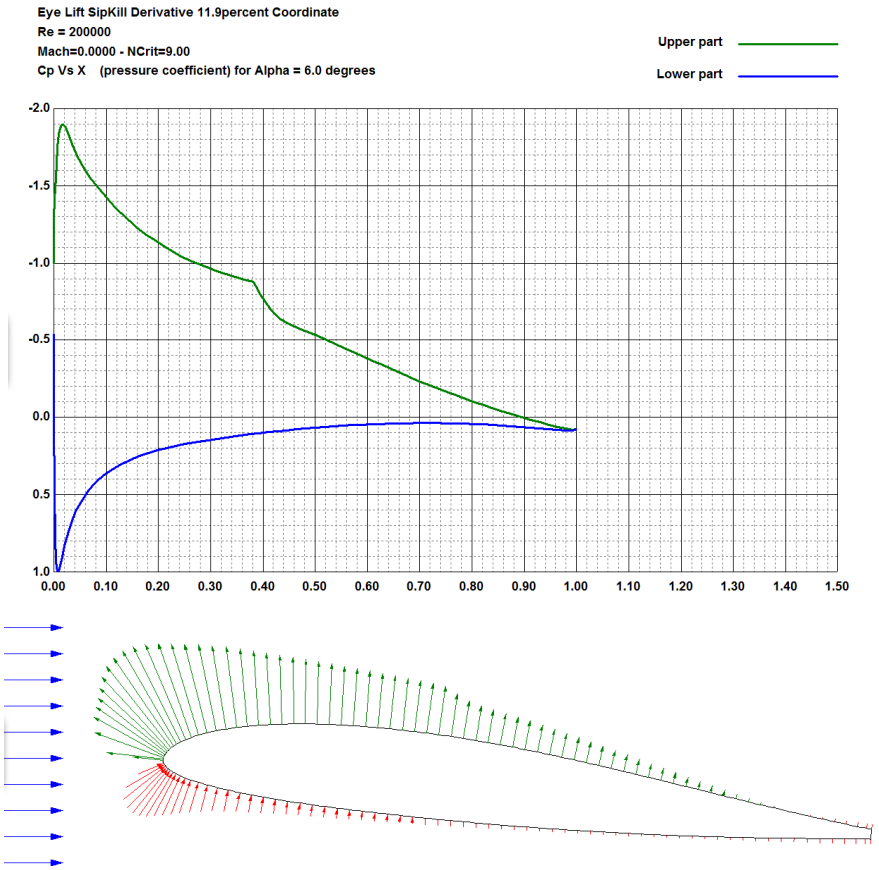

Figure 3. Cp versus X for Sipkill Derivative 11.9 percent airfoil

Lastly the propulsion system was addressed for ways in which it could be integrated in the most acoustically friendly way. To accomplish this a fairing was made for the motor to allow for aerodynamic flow around the motor while in flight and to allow for an installation that was restricted to the top side only. The propulsion system is required for launching the wing and gaining altitude but the glide ratio of the airframe is sufficient for powerless gliding. This capability was intent in the design and influenced the choice of the type of airframe. An additional design component to minimize airframe noise was to incorporate a folding propeller so that during powerless glides the propeller blades would fold back behind the fairing and have minimal interaction with the flow. Some of these features can be seen in figure 1.

4.2. Acoustic Sensor Array integration

The physical integration of the acoustic sensor array was also conducted under the guiding principle of minimization of any noise resulting from the physical presence of the sensor and its interaction with the flow. To accomplish this pod was designed and fabricated using the stereo lithography rapid prototyping process in which the data collection system and acoustic sensors were housed. A pocket was machined in the bottom side of the center section of the wing to accommodate the pod. The outer exposed skin of the pod was shaped such that it matched the airfoil shape of the center section in the location in which it was embedded. A rendering of the installation can be seen in figure 4.

The configuration of the acoustic array can also be seen in figure 4. One of the driving goals behind the measurements was to measure correlation lengths for directions in line with the flow and perpendicular to the flow. The positioning of the sensor locations can be seen to address this intent. In both directions the sensors were spaced 1.5 cm apart giving separation distances of 1.5 cm, 3.0 cm, and 4.5 cm with an additional spacing of 6 cm for the in line direction. The overall location of the array was chosen such that the in line row of sensors was close to the middle of the center section and the perpendicular row of sensors was far enough back from the leading edge to be in a region where the spatial variance in Cp was minimal over the dimensions of the array.

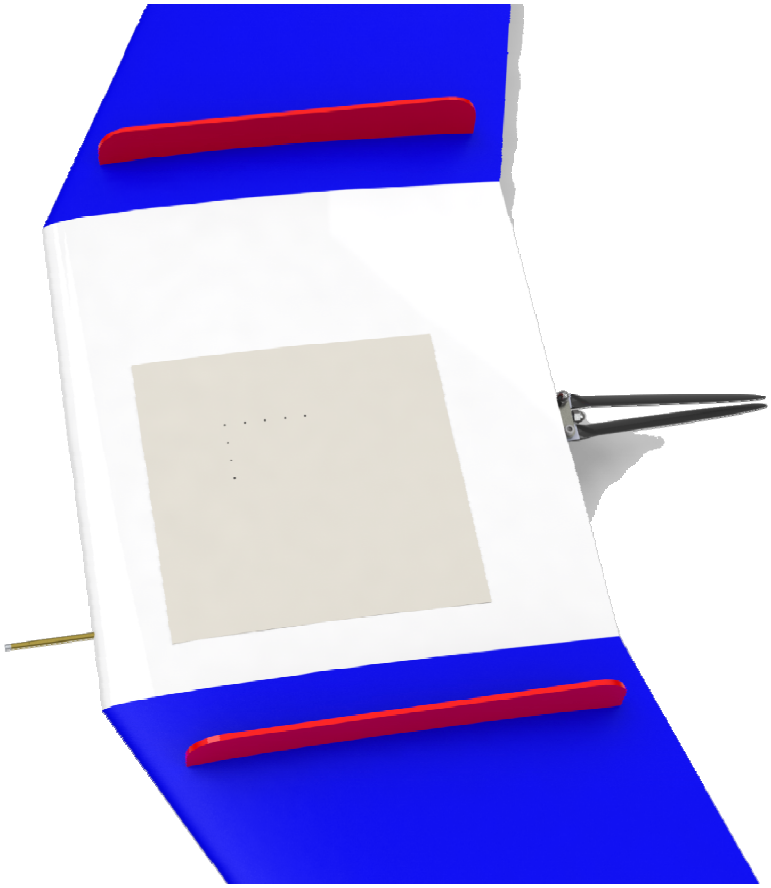

Figure 4. Embedded acoustic array in center section

4.3. Data Collection System

An acoustic system capable of performing the functions discussed above consists of several components. At the beginning of the signal path is a pressure transducer that is designed such that it responds to pressure variations on an acoustic scale (~ 1 Pascal maximum). The signal from the pressure transducer (microphone) is fed directly into a custom integrated circuit board integrated into the pod embedded in the center section of the flying wing. This board takes the electrical signal from the microphone and applies the necessary gain and then low pass filters it for anti aliasing purposes. The signal is then collected through an analog to digital converter and fed into the computer and stored with additional support data such as airspeed, temperature, altitude, etc..

The data collection system used for these experiments was custom designed and fabricated by Hyperion Technology Group, Inc.. The specifications for the system are as follows:

- Processor Board Size 4” x 4”.
- 8 channel, 24-bit synchronous Sigma-Delta analog-to-digital convertor.
- 128 KSPS max sample rate per channel.
- GPS receiver for data indexing and geo-location.
- GPS-disciplined master sample clock for data synchronization less than 1 microsecond.
- Digital compass for azimuth, roll, pitch, yaw and temperature.
- 600 MHz TI Overo Microprocessor.
- Linux Operating System.
- Wi-Fi, USB, and Bluetooth Connectivity.
- I2C connectivity for additional peripherals, such as airspeed, altitude, barometric pressure, humidity, etc…
- MicroSD card data storage.
- 2.4 GHz Zigbee Radio for Long-Range command and control up to 4 miles line-of-sight.
- 12 VDC supply, 3 W max with Wi-Fi enabled.

The integration into the pod and implementation of the acoustic sensors into the airfoil can be seen in figure 5. The physical size of the microphone module can be seen in the figure as referenced to a size of a dime. Pressure is measured by the acoustic sensors through a 0.025 inch hole giving access to the outside pressure through the skin of the airfoil. This configuration can also be seen in figure 5.

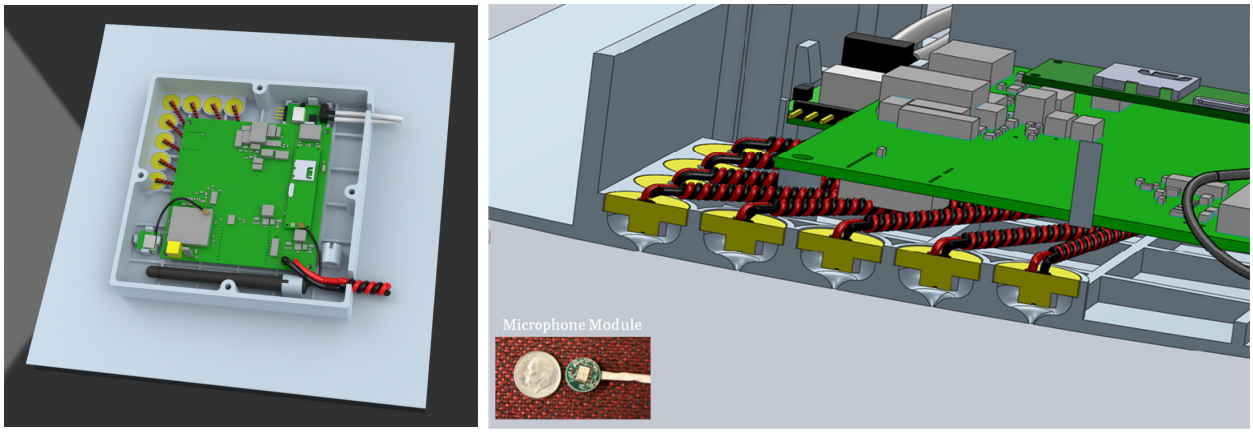

Figure 5. Data collection system installed in wing pod with sectional view of acoustic sensor implementation

5.0 Measurements and Results

5.1. Measurements

While data was collected during the entire flight of the flying wing only the two conditions of particular interest will be reported; 1) level flight with the engine in operation, 2) level flight in a steady glide condition with the engine off. A power spectral density plot of the noise as measured by three sensors on the flying wing while in flight can be seen in figure 6. The power spectral densities (PSD) are produced using 1 second of data resulting in 1 hertz bin widths and the levels are in dB re 20 μPa. This is done intentionally so that simple and direct comparisons can be made on tonal sound pressure levels (SPL). The result of displaying the data this way is that, for example, a 100 Hz tone with a level of 90 dB as measured by the acoustic sensor would result in a 90 dB level on the PSD plot (i.e. PSD units = Pa^2/Hz but since frequency width is 1 the level is equal to Pa^2). The net result of this is that a quick and simple rough comparison is afforded between a known source level and its expected signal to noise ratio as would be measured by the flying wing system as a function of distance between the source and receiver. When the data displayed in figure 6 was taken the flying wing was experiencing an airspeed of 8 m/sec and an altitude above the mean seal level (MSL) of 130 m. The PSD shown in figure 6 is an average over 5 PSDs which equates to 10 seconds worth of data. Although there were 7 functioning sensors in the system only 3 are shown to improve clarity in the plot by eliminating visual clutter. The three sensors chosen were the corner sensor and the sensor spaced 3 cm apart in each direction. This gives some indication of any possible differences resulting from spatial locations. It should not be assumed however that the differences in level displayed in this one plot are indicative of the differences in level experienced throughout the flight. There were instances of both greater and lesser differences but the scope of this report is not sufficient to cover these in detail.

An expected result that is noted in the data is a continual increase in the noise level toward lower frequencies. These results are intrinsic to the daytime atmosphere and are indicative of the well documented fact that the turbulent energy in the atmosphere is concentrated towards larger dimensional scales. Two additional items on the graph are worth note; first, there is a increase in the response in the range of 200 to 300 Hz. This hump in the response tracks fairly well with the airspeed in both level and frequency in the sense that the level and frequency both increase if the airspeed increases. Due to some preliminary analysis it is speculated that this is aeroacoustic in nature and appears to come from the rear of the aircraft. It is hoped that further analysis of the date will help identify the source of this contribution to the noise. Secondly, there is a dip in the noise level slightly above 600 Hz or there are humps in the noise level on both sides of this frequency. This feature is not as prevalent and consistently defined as the previous and there are no speculative reasons for its existence defined as of yet.

As discussed in section 2.2 above the noise as measured by the acoustic sensors contains pressure fluctuations inherent in the turbulent atmosphere as well as fluctuations due to flow interactions with the airframe and sensor body. With a single sensor it is not possible to separate these two since both are pressure fluctuations therefore it is not an easy task to know when the flow interaction noise has been reduced below the atmospheric noise. This point is important because it indicates when further improvements to the airframe or windscreen will not produce improvements to the measured noise floor. Theoretical predictions have been attempted to determine this number but to our knowledge it has not been experimentally verified from an aerial platform. Without prior knowledge of these values about the only experimental path that can be pursued is to continually make airframe and windscreen improvements until the measured noise no longer decreases. This approach is obviously not very efficient since so many variables exist in this area of study.

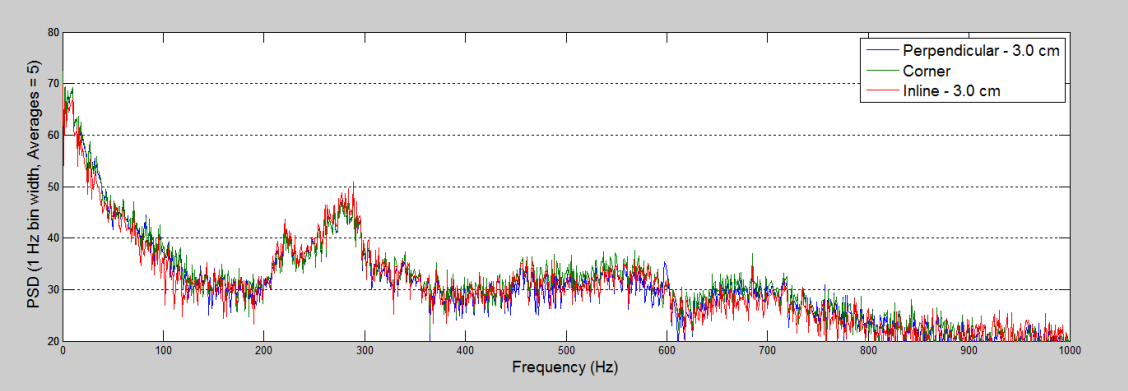

Figure 6. PSD of noise measured by acoustic sensors on flying wing at an airspeed of 10 m/sec and an altitude of 114 m above MSL.

An additional state of the system considered was when the propulsion system on the flying wing was in operation. A PSD of one of these instances can be seen in figure 7. As expected the noise floor level is substantially higher but also very tonal in nature. The propulsion system employed on the flying wing is somewhat similar in design to what is used on the small class of electric UAVs but no consideration was given to procedures or design elements that would reduce the noise level emitted by the propulsion system while in operation.

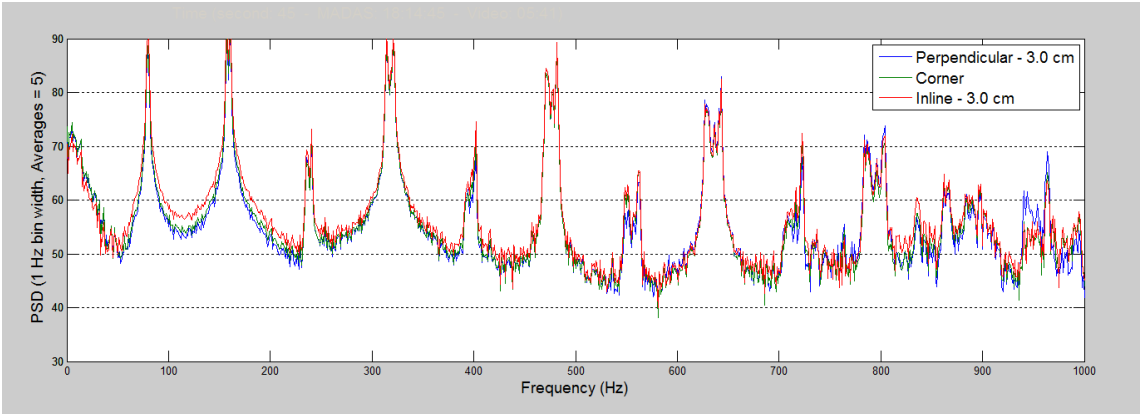

Figure 7. PSD of noise measured by acoustic sensors on flying wing at an airspeed of 7 m/sec and an altitude of 115 m above MSL with the engine in operation.

5.2. Results

The SNR of a measured signal and the system noise determines its detectability such that once the signal is low enough that the SNR has reached some minimum value the signal can no longer be dependably detected. Because acoustic waves are attenuated as they propagate through the atmosphere the detection range is roughly determined by the initial level of the source and the noise as measured by the acoustic sensor system. At the most basic level a useful approximation of detection distance can be determined by taking the difference in dB between the source level at 1 meter at a particular frequency and the noise level of the detection system at this same frequency and converting it to a distance (e.g. 60 dB difference = 1 kilometer detection range). In this simple analysis the only attenuation method accounted for is spherical spreading and no particular detection schemes are taken into account therefore depending on the robustness of the signal processing of the system and the actual propagation environment the actual results may be better or worse than this simple approximation. For example considering the results in figure 6 this approximation would indicate that a 90 dB 400 Hz source could be detected at a distance of 1 kilometer.

6.0 References

1. Crighton, D. G. 1991 Airframe noise. Chapter 7 in Hubbard, H. H., ed., "Aeroacoustics of Flight Vehicles, Theory and Practice--Volume 1: Noise Sources," NASA Reference Publication RP-1258-VOL1, pp. 391-447.
2. Farassat, F. 1975 Theory of Noise Generation from Moving Bodies with an Application to Helicopter Rotors. *NASA Technical Report (TR) R-451, Langley Research Center, Hampton, VA 23665, December 1975.*
3. Farassat, F. and Casper, J. 2003 Some Analytic Results for the Study of Broadband Noise Radiation from Wings, Propellers and Jets in Uniform Motion. *International Journal of Aeroacoustics, Vol. 2, No. 3 & 4, 2003, pp. 335 – 350.*
4. Farassat, F. and Myers, M. K. 1986 Aerodynamics via Acoustics: Application of Acoustic Formulas for Aerodynamic Calculations. *AIAA Paper No. 86-1877, presented at the AIAA 10th Aeroacoustics Conference, July 9-11, 1986.*
5. Farassat, F. and Posey, J. W. 2003 The Role of Analytic Methods in Computational Aeroacoustics. Aerospace Numerical Simulation Symposium 2003 National Aerospace Laboratory, Tokyo, Japan, 12 June 2003.
6. Hardin, J. C., Fratello, D. J., Hayden, R. E., Kadman, Y., and Africk, S. 1975 Prediction of Airframe Noise. *NASA Technical Note TN D-7821, February 1975.*
7. Lighthill, M. J. 1978 Waves in Fluids. *New York: Cambridge University Press.*
8. Lilley, G. M. 2001 The Prediction of Airframe Noise and Comparison with Experiment. *J. Sound Vib., vol. 239, no. 4 (April 2001), pp. 849-859.*
9. Lockard, D. P., and Lilley, G. M. 2004 The Airframe Noise Reduction Challenge. *NASA/TM–2004–213013, April 2004.*
10. Morgan, S. and Raspet, R. 1992 Investigation of the Mechanisms of Low-Frequency Wind Noise Generation Outdoors. *J. Acoust. Soc. Am. 92 (2), Pt 1, August 1992, pp 1180-1183.*
11. Smith, A. M. O. and Bauer, A. B. 1970 Static-Pressure Probes That Are Theoretically Insensitive to Pitch, Yaw and Mach Number. J. Fluid Mech. Vol. 44, part 3, pp. 513-528.